Physics Letters A 441 (2022) 128163

Contents lists available at ScienceDirect

Physics Letters A

www.elsevier.com/locate/pla

The effect of doping $MoSe_2$ by clusters of noble metals on its adsorption for NH_3

Ahmad I. Ayesh

Physics Program, Department of Mathematics, Statistics and Physics, College of Arts and Science, Qatar University, P.O. Box 2713, Doha, Qatar

ARTICLE INFO

Article history:
Received 13 February 2022
Received in revised form 21 April 2022
Accepted 22 April 2022
Available online 26 April 2022
Communicated by M. Wu

Keywords:
$MoSe_2$
Trimer
NH_3
DFT
Pt
Au

ABSTRACT

The development of industrial activities is associated with negative impacts on the quality of the environment including emission of hazardous gases. Therefore, it is critical to produce sensitive and selective gas detectors in order to monitor and maintain its good quality. This work investigates the effect of noble metal doping of $MoSe_2$ on its adsorption of ammonia (NH_3) gas. Pristine and noble metal doped $MoSe_2$ structures are examined computationally using density functional theory (DFT). Clusters of timers of each Pt, Au, and Ag along with their combination are utilized for doping. The influence of doping $MoSe_2$ structure on its adsorption energy and distance of NH_3 gas, density of states (DOS), charge transfer between NH_3 and the $MoSe_2$ structures, and band structure is explored. When compared to the pristine structure, the doped $MoSe_2$ structures reveal significant changes in electronic characteristics that are reflected on the DOS and band structures. New energy bands have evolved near to the Fermi level because of modifying the $MoSe_2$ structure. The adsorption capacity of the doped structures is greatly enhanced due to incorporation of noble metals. Herein, the magnitude of adsorption energy increases and the adsorption distance deceases for NH_3 gas. Consequently, the sensitivity is improved in comparison to the pristine structure. This study shows that noble metal doping of $MoSe_2$ by clusters of trimers can be a useful approach for developing sensitive NH_3 gas detectors.

1. Introduction

The growth of industrial and agricultural functions is linked with increasing the emissions of harmful gases, such as: nitrogen oxide (NO), carbon monoxide (CO), carbon dioxide (CO_2), and ammonia (NH_3) [1,2]. NH_3 is a general chemical that is needed for different agricultural and industrial applications, and it is also generated as a waste from multiple agricultural and industrial processes [3]. However, it is a very toxic gas to human along with its negative impact on the environment [4]. The exposure limit of ammonia to human health should not exceed 50 ppm for safe work sites, nevertheless, its long-term indoor exposure should not exceed 25 ppm [5]. Exceeding the exposure limits of ammonia on the long term may cause severe influence on human health that include: injuries, risky burns, harmful effects on the respiratory system, and eye irritation [6]. Consequently, the development of precisely sensitive and selective NH_3 sensors to maintain a safe work environment is crucial, especially in sectors involving NH_3 production units, the industry of agricultural fertilizers, and food processing companies.

Transition metals of two dimensional (2D) are recognized for their outstanding properties which can be used in numerous fields of applications [7,8]. Production of chemical sensors is one of these fields where they make use of the enormous reactivity that is allocated to the high concentration of reactive cites produced by the vast surface area of 2D structures [9,10]. Molybdenum disulfide ($MoSe_2$) 2D nanostructure is a dichalcogenide semiconductor with eminent electrical and structural features [11]. Hence, it is usable for a diversity of applications inclusive of gas sensors [12]. A monolayer of $MoSe_2$ composes of layers of each Se and Mo, where the Mo layer is sandwiched between two Se layers. Each Se atom is linked by six Mo atoms through covalent bonds [13,14]. $MoSe_2$ 2D monolayer is characterized by its direct bandgap of $E_g \cong 1.6$ V, unlike its bulk equivalent that displays an indirect bandgap [15]. Furthermore, because of its large surface area, $MoSe_2$ 2D nanostructure has exceptional catalytic activity, and its electrical characteristics are boosted by the electrocatalytically active unsaturated Se atoms near the edges [16]. As a result, $MoSe_2$ monolayer is seen as a promising structure for a variety of applications, including gas detection [17,18].

Recently, several research groups have been looking at the use of $MoSe_2$ in a variety of applications, including energy storage, catalysis, optoelectronics, and gas and chemical sensors. [19,20].

E-mail address: ayesh@qu.edu.qa.

https://doi.org/10.1016/j.physleta.2022.128163

For example, $MoSe_2$ was considered for its use to fabricate battery electrodes, and it was changed to lessen its conductivity with the goal of increasing its efficiency [21]. Y. Kim et al. investigated 2D MoS_2 for gas sensor of NO_2 by controlling the height of Schottky barrier [22]. The structure was fabricated by chemical vapor deposition at low temperature to achieve the structure. Then, the Schottky barrier height was varied by selecting different types of electrode materials. Increasing the Schottky barrier height, increases the NO_2 responsivity. Y. Gui et al. modified $MoSe_2$ by Au atom as well as its clusters and tested its features for adsorption of C_2H_4 gas using density functional theory (DFT) investigation [23]. They found that the adsorption capacity of doped $MoSe_2$ for C_2H_4 gas can be sorted as $Au_3 > Au_2 > Au > Au_4$ for a single C_2H_4 molecule. Furthermore, subsequent to C_2H_4 adsorption, both Au and Au_4 doped structures had enhanced conductivity, while the Au_2 and Au_3 structures had reduced conductivity. Y. Gui et al. also explored the adsorption of C_2H_2 on $MoSe_2$ monolayer decorated by Pt nanoclusters using DFT calculation [24]. They reported that an oversized Pt nanocluster might generate an antibonding orbit located near the Fermi level. The Pt_{13} decorated $MoSe_2$ structure has a decent adsorption to C_2H_2 where it caused sp^2 hybridized. H. Luo et al. examined the adsorption characteristics of both NO_2 and NH_3 molecules on $MoSe_2$ modified by doping with P, Al, and Si atoms using DFT calculation [25]. They illustrated that the modified structures have improved adsorption compared with the unmodified $MoSe_2$ structure. Besides, the modification increases the impact of orbital hybridization of the gas on the $MoSe_2$ structure, and promotes charge transfer.

First principles DFT analysis are used to investigate the effect of noble metal doping of $MoSe_2$ 2D structure on its adsorption capacity for NH_3 gas. Trimers of each gold, platinum, and silver are used as clusters to dope $MoSe_2$ as well as their combination. The metals are selected due to their high affinity to NH_3 gas. Clusters of three atoms are utilized since this will modify a single cell of $MoSe_2$ structure, thus, it is expected to reveal high adsorption [23]. The investigation involves examining the effect of doping on band structure, DOS, bandgap energy, adsorption distance and energy, and change in the charge of NH_3 molecule upon its adsorption. Doping of $MoSe_2$ causes significant variations in its electronic characteristics and improves its adsorption of ammonia.

2. Computational method

DFT computations were used to explore the effect of noble metal doping of $MoSe_2$ structure on its adsorption of the NH_3 molecule [26,27]. An atomistic quantum (ATK) simulation software package produced by Synopsys was employed to investigate the electronic characteristics, band structure, as well as adsorption parameters [26,28–30]. A 5×5 supercell of $MoSe_2$ was built then doped with trimer clusters of each Au, Pt, and Ag as well as their combination. Herein, three dopant atoms of one type or the combinations substituted the central Se atoms. It should be noted that the adatom process could be established by replacement of an atom (doping), or introduction of an atom on either of a bridge site or at the center of the ring. The doping was selected for this investigation since it is expected to result in higher adsorption energy, since the other two options reduce the number of free bonds that negatively impact the adsorption of ammonia [31]. The new structures were labeled as: $MoSe_2$+Pt_3, $MoSe_2$+Au_3, $MoSe_2$+Ag_3, and $MoSe_2$+Pt-Au-Ag. The effect of doping is a surface effect since the present structure in a mono layer of $MoSe_2$, and the doping cite is selected in the middle of the structure to reduce the edge effect. The generalized gradient approximation (GGA) associated with the Perdew B. Ernzerh (PBE) exchange correlation was employed to examine the electron exchange correlation [32,33]. The impact of Van der Waals force was adjusted using the DFT-D2 Grimme function [33]. The spin effect is ignored for the doping atoms since it is expected to be minimal at room temperature for low concentration of dopants (one to three atoms) and since magnetic features are not the focus of this work [34]. All structures were optimized at 100 Hartree cutoff energy mesh and a 300 K temperature. The resolution of stress and force tolerance throughout the optimization were 0.1 GPa and 0.01 eV/Å, respectively. A grid of the Monkhorst Pack Brillouin zone was employed to select the k-point sampling of $4 \times 4 \times 1$ which was applied to all optimization computations, i.e. electronic characteristics and geometry [35].

Table 1
Bandgap of pristine and doped $MoSe_2$ structures.

Structure	E_g (eV)
$MoSe_2$	1.609
$MoSe_2$+Pt_3	0.551
$MoSe_2$+Au_3	0.162
$MoSe_2$+Ag_3	0.242
$MoSe_2$+Pt-Au-Ag	0.283

For each structure, the ammonia molecule was placed above the doping site and it was free to move and to rotate. The optimum adsorption site was identified upon optimization of the structure. The gas adsorption energy ($E_{Ads.}$) on each $MoSe_2$ structure was calculated by the equation [2,36,37]:

$$E_{Ads.} = E_{MoSe_2+gas} - (E_{MoSe_2} + E_{gas}) \quad (1)$$

Where E_{MoSe_2+gas} represents the total energy for a $MoSe_2$ structure with NH_3 adsorbed, E_{MoSe_2} is the total energy for a $MoSe_2$ structure, and E_{gas} is the total energy for NH_3 molecule. The Mulliken population scheme was utilized to compute the charge transferred (Δq) among NH_3 and a $MoSe_2$ structure post its adsorption as [37,38]:

$$\Delta q = q_a - q_b \quad (2)$$

Where, q_a and q_b refer to the total Mulliken charge for the gas molecule subsequent and prior its adsorption, respectively. The investigation also involved the evaluation of the effect of gas adsorption on DOS, the energy of bandgap (E_g), and distance between the ammonia molecule and the structure (d) known as the adsorption distance for all $MoSe_2$ structures.

3. Results and discussion

The adsorption of ammonia gas on pristine and noble metal doped $MoSe_2$ structures is explored in this investigation. Monolayers of $MoSe_2$+Pt_3, $MoSe_2$+Au_3, $MoSe_2$+Ag_3, and $MoSe_2$+Pt-Au-Ag structures are constructed and optimized as shown in Fig. 1. The length of Se-Mo bond is 2.58 Å in all constructed $MoSe_2$ structures. The bond lengths for the doped structures are Mo-Pt, Mo-Au, and Mo-Ag within the mono-doped structures are 2.60, 2.69, and 2.79 Å, respectively. However, the bond lengths of Mo-Pt, Mo-Au, and Mo-Ag for the co-doped structure are 2.57, 2.67, and 2.84 Å, respectively.

Introducing a dopant to $MoSe_2$ structure modifies its energy levels and consequently the energy band structure. Fig. 2 displays the energy band structures for $MoSe_2$, $MoSe_2$+Pt_3, $MoSe_2$+Au_3, $MoSe_2$+Ag_3, and $MoSe_2$+Pt-Au-Ag. The main feature observed in the figure is that doping of a structure generates new levels of energy. The values of bandgap energies for all $MoSe_2$ structures are identified as shown in Table 1. The pristine $MoSe_2$ structure has a direct bandgap, and its energy is 1.609 eV (i.e. typical semiconductor) and it is in agreement with recent experimental and

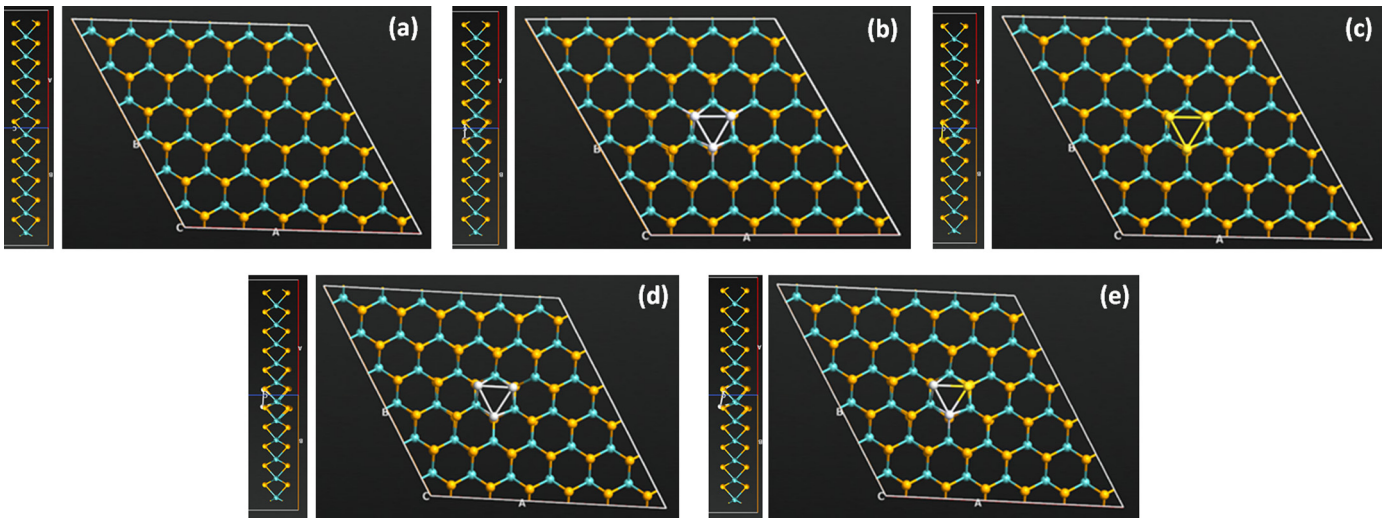

Fig. 1. The optimized $MoSe_2$ structures (top and side views) of: a) pristine $MoSe_2$, b) $MoSe_2$+Pt_3, c) $MoSe_2$+Au_3, d) $MoSe_2$+Ag_3, and e) $MoSe_2$+Pt-Au-Ag.

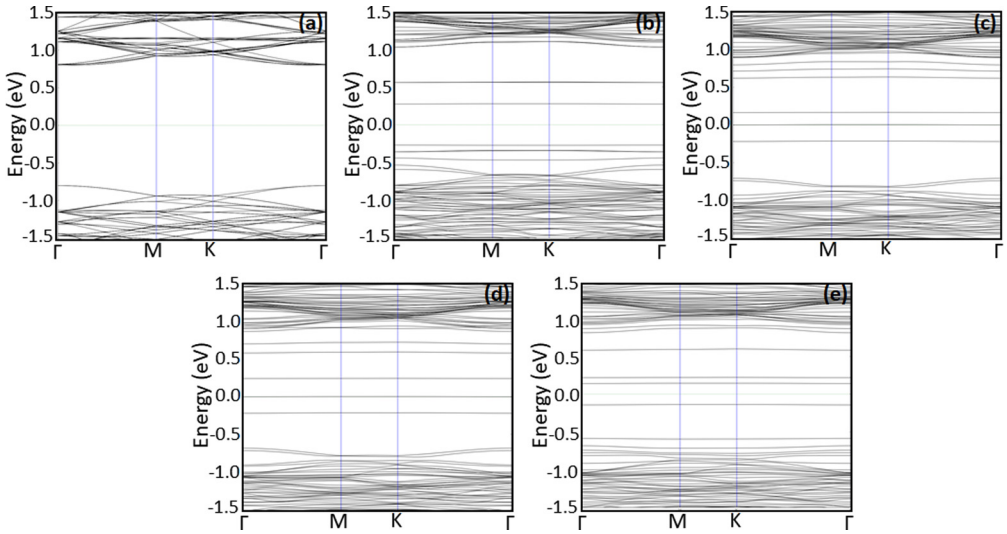

Fig. 2. The band structures for the optimized pristine as well as doped $MoSe_2$ structures: a) pristine $MoSe_2$, b) $MoSe_2$+Pt_3, c) $MoSe_2$+Au_3, d) $MoSe_2$+Ag_3, and e) $MoSe_2$+Pt-Au-Ag.

computational findings [39,40]. Introducing a dopant within the lattice structure of $MoSe_2$ reduces the bandgap energy. In particular, the $MoSe_2$+Au_3 structure has the minimum bandgap energy; the $MoSe_2$+Pt_3 structure has the maximum bandgap energy for the doped structures, while the $MoSe_2$+Ag_3 and $MoSe_2$+Pt-Au-Ag structures have moderate bandgaps.

Fig. 3 reveals the optimized structures of $MoSe_2$+Pt_3, $MoSe_2$+Au_3, $MoSe_2$+Ag_3, and $MoSe_2$+Pt-Au-Ag subsequent to adsorption of NH_3 gas. The figure demonstrates the chemisorption (establishment of chemical bonds) of NH_3 gas on all structures except the pristine and the $MoSe_2$+Ag_3 structures where no bonds are observed. This specifies that the $MoSe_2$+Pt_3, $MoSe_2$+Au_3, and $MoSe_2$+Pt-Au-Ag structures exhibit more potential for NH_3 gas adsorption. Table 2 illustrates the adsorption distance for NH_3 gas on the pristine and doped structures. The minimum adsorption distance is for the $MoSe_2$+Pt_3 structure, while the pristine structure exhibits the maximum adsorption distance. The $MoSe_2$+Au_3, $MoSe_2$+Pt-Au-Ag, and $MoSe_2$+Ag_3 structures have almost similar adsorption distances of ∼0.23 Å. Those results are in qualitative agreement with the observation of chemisorption of NH_3 in Fig. 3. Furthermore, the $MoSe_2$+Au_3, and $MoSe_2$+Ag_3 structures exhibit average adsorption distances.

Table 2
Bandgap energy, adsorption energy and distance, and charge transferred among NH_3 and $MoSe_2$ structures upon its adsorption.

Structure	E_g (eV)	$E_{Ads.}$ (eV)	d (Å)	Δq (e)
$MoSe_2$+NH_3	1.600	−0.315	2.78	−0.032
$MoSe_2$+Pt_3+NH_3	0.730	−1.181	2.210	−0.197
$MoSe_2$+Au_3+NH_3	0.233	−0.941	2.300	−0.195
$MoSe_2$+Ag_3+NH_3	0.292	−0.851	2.300	−0.192
$MoSe_2$+Pt-Au-Ag+NH_3	0.255	−0.954	2.280	−0.204

The band structures of the $MoSe_2$+Pt_3, $MoSe_2$+Au_3, $MoSe_2$+Ag_3, and $MoSe_2$+Pt-Au-Ag monolayers after adsorption of NH_3 molecules are presented in Fig. 4. New subbands appear within the valence and conduction bands due to NH_3 gas adsorption which modifies the band structures. The bandgap energies of all structures after adsorption of NH_3 gas are presented in Table 2. Except the pristine and $MoSe_2$+Pt-Au-Ag structures, the bandgap energy increases slightly after adsorption of NH_3 gas. Fig. 4 also illustrates some dissimilarities in DOS after gas adsorption (as compared with Fig. 2) as discussed further below [41].

The cluster doping with trimers of a $MoSe_2$ structure noticeably enhances its adsorption of ammonia as illustrated in Table 2.

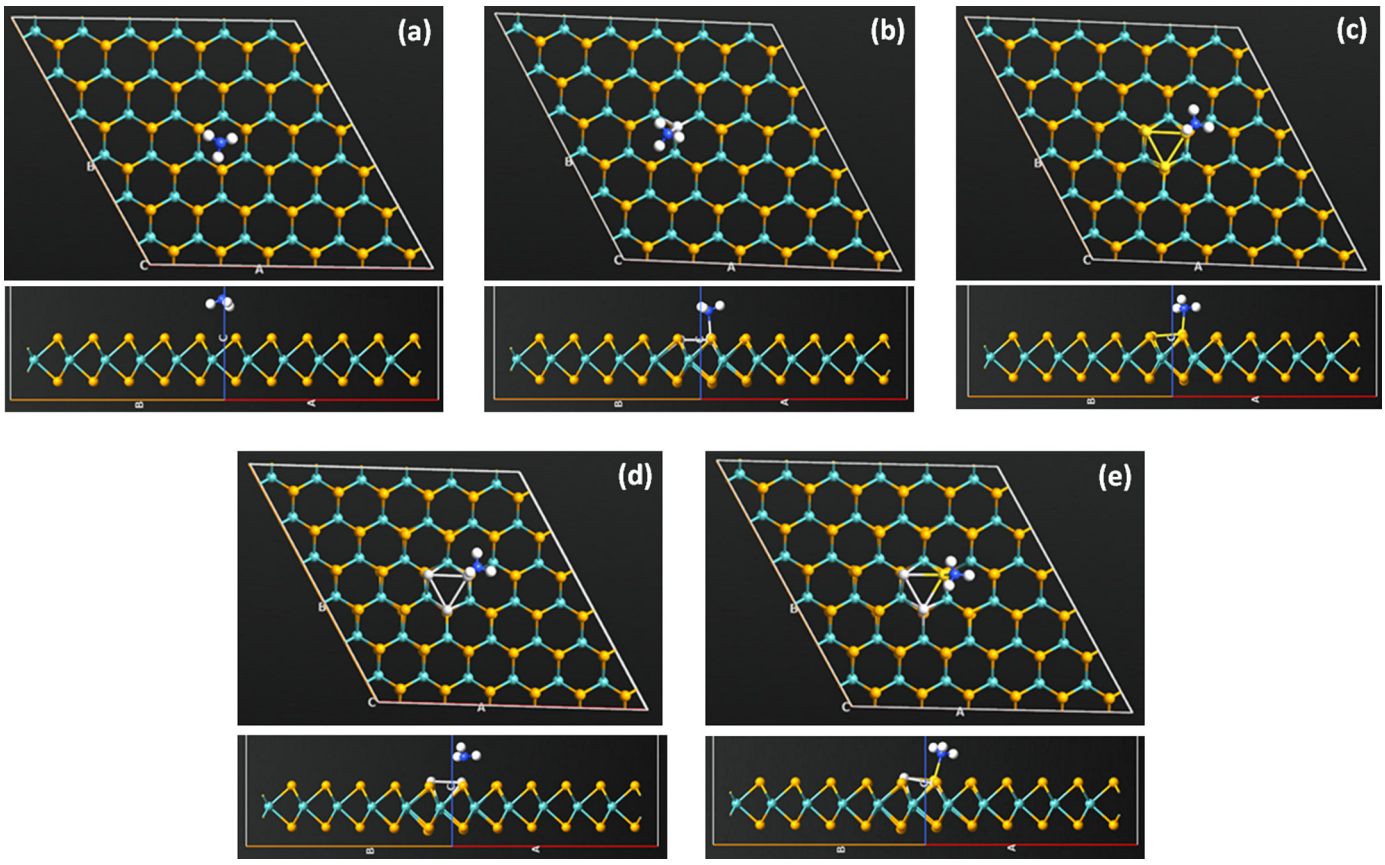

Fig. 3. The optimized $MoSe_2$ structures (top and side views) after NH_3 adsorption: a) pristine $MoSe_2$, b) $MoSe_2$+Pt_3, c) $MoSe_2$+Au_3, d) $MoSe_2$+Ag_3, and e) $MoSe_2$+Pt-Au-Ag.

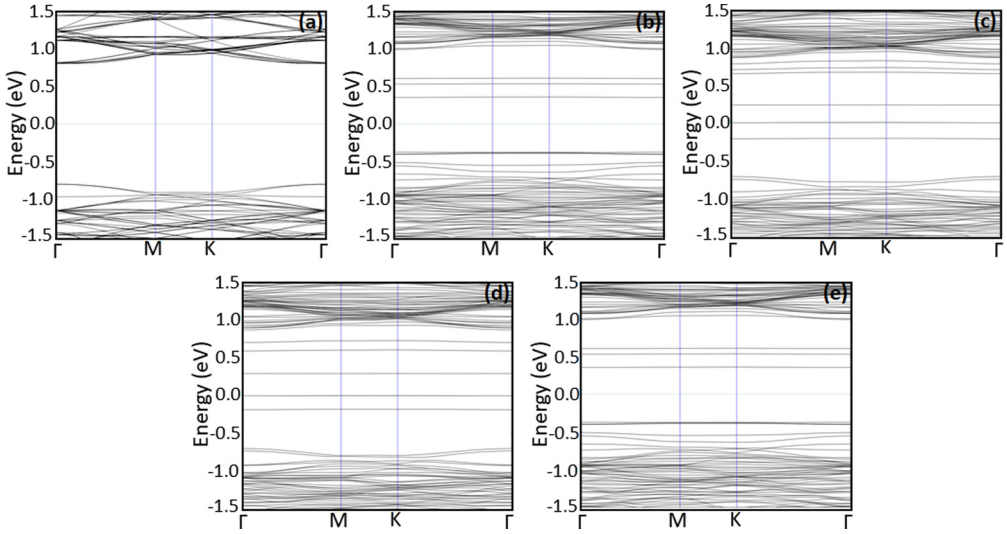

Fig. 4. The band structures for the optimized pristine as well as doped $MoSe_2$ structures after NH_3 adsorption: a) pristine $MoSe_2$, b) $MoSe_2$+Pt_3, c) $MoSe_2$+Au_3, d) $MoSe_2$+Ag_3, and e) $MoSe_2$+Pt-Au-Ag.

The adsorption energy here indicates the capacity of a structure for application as a NH_3 gas sensor. Table 2 reveals that doping of $MoSe_2$ structure with trimers increases the magnitude of its adsorption energies. The $MoSe_2$+Pt_3 structure has the maximum magnitude of adsorption energy, while the minimum is for the pristine structure. Furthermore, the $MoSe_2$+Ag_3 structure has the minimum magnitude of adsorption energy among the doped structures. The magnitudes of adsorption energies of both $MoSe_2$+Au_3 and $MoSe_2$+Pt-Au-Ag are average in magnitude and almost similar, i.e. ~ -0.95 eV. The adsorption energy in the table is negative, indicating that the doped structures have a strong adsorption of NH_3 gas and that charges have been transferred to it [27].

The charge transferred from the NH_3 gas is presented in Table 2, and its maximum magnitude is for the $MoSe_2$+Pt_3 structure while the minimum is for the pristine structure. The $MoSe_2$+Au_3, $MoSe_2$+Ag_3, and $MoSe_2$+Pt-Au-Ag have average magnitudes of charge transferred of around ~ -0.2 e. The negative value of charge transferred indicate that charges are transferred from the NH_3 gas to the $MoSe_2$ structures. The values of charge transferred are consistent with those of the adsorption energies. Accordingly,

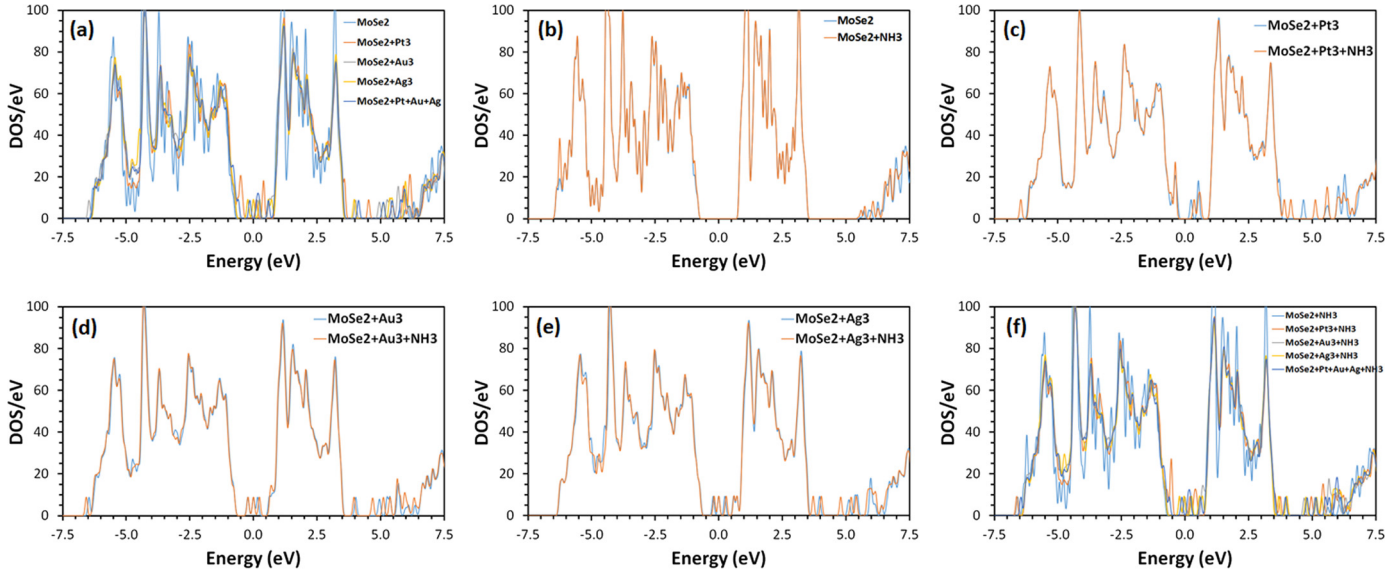

Fig. 5. DOS for the optimized pristine and doped $MoSe_2$ structures prior to NH_3 adsorption (a); and DOS prior and post to NH_3 adsorption for: b) pristine $MoSe_2$, c) $MoSe_2$+Pt_3, d) $MoSe_2$+Au_3, e) $MoSe_2$+Ag_3, and f) $MoSe_2$+Pt-Au-Ag. (For interpretation of the colors in the figure, the reader is referred to the web version of this article.)

it can be concluded that $MoSe_2$+Pt_3 structure has the highest capacity for ammonia adsorption, followed by the $MoSe_2$+Pt-Au-Ag structure and then $MoSe_2$+Au_3. It should be noted that the $MoSe_2$+Ag_3 structure has low capacity of ammonia adsorption since no chemisorption is observed. Furthermore, the pristine structure is the least desirable structure for NH_3 gas adsorption because of its minimum adsorption energy, maximum adsorption distance, and no chemisorption of the molecule [42–44]. The adsorption energy magnitude of NH_3 on $MoSe_2$+Pt_3 structure is 3.75 times higher than that of the undoped structure. Accordingly, the $MoSe_2$+Pt_3 structure can be proposed as an efficient system for fabrication of sensitive ammonia sensors. Here, cluster doping with the noble metals of $MoSe_2$ structures can be an efficient approach for enhancement of ammonia adsorption. This inference is in agreement with latest research [17,19]. The noble metals of Pt, Au, and Ag modify the levels of energy of $MoSe_2$ monolayers and improve their interaction with ammonia near the doping site [18].

The influence of cluster doping of $MoSe_2$ on the density of states of both bands (valance and conduction) is presented in Fig. 5(a). The figure illustrates that the trimer doping of $MoSe_2$ with of Pt, Au, and Ag alters the DOS. In general, the intensity of DOS is reduced as a result of doping as observed, for example, at 1.14, 1.49, 1.70, 203, 3.18, −1.43, −2.08, and −3.75 eV. New bands are introduced close to the Fermi level that modify bandgap energy of the structures such as the bands at −0.53, −0.23, −0.12, 0.11, 0.17, 0.43, and 0.63 eV. The DOS of pristine $MoSe_2$ does not have, in general, major changes due to NH_3 adsorption as shown in Fig. 5(b). This can be rationalized since NH_3 molecule is physisorbed on the $MoSe_2$ structure. On the other hand, adsorption of ammonia on doped $MoSe_2$ structures causes noticeable alteration in the intensity of DOS (compared to DOS before adsorption) at some energy levels, as presented in Figs. 5(c) – 5(f). In particular, clear alterations due to ammonia adsorption on doped $MoSe_2$ structures are observed close to the Fermi level such as those at: 0.56, 0.22, −0.01, −0.07 eV for the $MoSe_2$+Pt_3, $MoSe_2$+Au_3, $MoSe_2$+Ag_3, and Pt-Au-Ag-$MoSe_2$ structures, respectively. The adjustments to the bandgaps (Fig. 4 and Table 2) are justified by the new DOS peaks for doped $MoSe_2$ structures. The figure reveals that adsorption of ammonia on doped $MoSe_2$ structures does not cause dramatic changes in the general shape of DOS. Furthermore, the intensity of DOS within the valance band is higher, in general, than that within the conduction band for all structures. Accordingly, one can conclude that the noble metal doping and NH_3 gas adsorption are the reasons for the new alterations observed in DOS in Fig. 5.

The new alterations in DOS are assigned to the quantum confinement that influences charge carriers and energy level hybridization (between d and s levels) of the two atoms, molybdenum and selenium. Here, electric charges are transferred from the NH_3 gas to the $MoSe_2$ structures, which alter the DOS near the Fermi level and move charges to the p level of energy for selenium. The Fermi level, which determines the hole doping for the $MoSe_2$ structure, is shifted due to adsorption of NH_3 gas. Orbital hybridization caused by ammonia adsorption on $MoSe_2$ structures is nearby the Fermi level as presented by Fig. 5. Pristine and doped $MoSe_2$ structures exhibit nearly flat bands signifying the up spin states for ammonia gas close to the Fermi level that result in its strong adsorption. The main source of alteration for $MoSe_2$ structures is the occupied energy states of DOS following to NH_3 gas adsorption [45]. Consequently, the results demonstrate that cluster doping with noble metals of $MoSe_2$ advances their adsorption efficiency for ammonia gas.

S. Singh et al. exemplified the effective use of the $MoSe_2$ nanostructure for NH_3 sensor experimentally [12]. They showed that the nanostructure can be used efficiently at room temperature for ammonia detection with precise sensitivity for 10 ppm of the gas. As the sensor was subjected to NH_3, its resistance increased exemplifying that the $MoSe_2$ structure exhibited p-type characteristic. The enhancement of the gas response was imputed to the transfer of electrons from NH_3 to $MoSe_2$, which resulted in a drop in hole concentration of the $MoSe_2$ (p-type semiconductor), raising its resistance of (the $MoSe_2$ channel) as illustrated by the band gap energy after adsorption of NH_3 in Table 2. Additionally, the increase in the $MoSe_2$ sensor response against NH_3 gas consequent to modification by noble metals was demonstrated, and assigned to the increase in gas adsorption efficiency due to the extraordinary reactivity as well as affinity of the noble metals towards ammonia gas [46].

The sensor response (SR) of a gas sensor can be calculated using [47]:

$$SR = \left| \frac{\rho_a - \rho_b}{\rho_b} \right| \tag{3}$$

Table 3
The calculated sensor response of $MoSe_2$ structures towards NH_3 according to Eqs. (3) and (4).

Structure	Sensor Response (SR)
$MoSe_2$+NH_3	0.16
$MoSe_2$+Pt_3+NH_3	30.85
$MoSe_2$+Au_3+NH_3	2.95
$MoSe_2$+Ag_3+NH_3	1.63
$MoSe_2$+Pt-Au-Ag+NH_3	0.42

Where ρ_b and ρ_a refer to the resistivities prior and post to ammonia adsorption, respectively, and can be evaluated using [17]:

$$\rho = \rho_0 e^{\frac{E_g}{2k_B T}} \tag{4}$$

Where ρ_0 represents a temperature-independent constant (ρ_0 is eliminated in Eq. (3) since it is a ratio), T is the $MoSe_2$ sensor temperature in Kelvin and it is set to 300 K, E_g is the energy of bandgap, and the Boltzmann constant $k_B = 8.62 \times 10^{-5}$ eV.K^{-1}. Table 3 shows the calculated response, according to Eqs. (3) and (4). The table shows that the maximum response is for the $MoSe_2$+Pt_3 structure while the minimum is for the pristine structure. The next highest response is for the $MoSe_2$+Au_3 structure. The $MoSe_2$+Ag_3 structure exhibits a relatively low response. Those results are in qualitative consent with the computed adsorption energy and distance as well as charge transferred. The outstanding gas response values, validate the exceptional enhancement for NH_3 gas adsorption due to doping ($\sim$192 times for $MoSe_2$+Pt_3 as compared with the pristine structure) that advocate the DFT computations. The only discrepancy is related to the low response of $MoSe_2$+Pt-Au-Ag structure, however, the presented values of response are estimations. The cluster doping of $MoSe_2$ structure with noble metals can be considered for sensitive detection of ammonia gas with the best sensitivity is for the $MoSe_2$-Pt_3 structure.

4. Conclusion

The effect of cluster doping for $MoSe_2$ structure on its adsorption of ammonia (NH_3) gas has been researched by density functional theory (DFT) first principles calculations. The gas adsorption capacity was assessed by evaluation of ammonia adsorption distance and energy as well as charge transported from/to NH_3, along with the density of states (DOS) and band structure of $MoSe_2$. The cluster doping of $MoSe_2$ structure was established by substitution of three selenium atoms by trimers of each Pt, Au, and Ag, along with their combination Pt-Au-Ag. The doping generated significant alterations of energy band structure. The bandgap of $MoSe_2$ structure was reduced because of doping, and few energy bands were introduced within the DOS. Doping of $MoSe_2$ structures improved their adsorption capacity for ammonia gas where it increased the magnitude of adsorption energy, reduced the adsorption distance, increased the magnitude of charge transported from NH_3 to $MoSe_2$, and resulted in chemisorption of NH_3 on $MoSe_2$. The investigation suggested that the $MoSe_2$+Pt_3 structure has the best adsorption capacity for ammonia by 3.75 times as compared with the pristine structure. The findings of this investigation show that the Pt_3 doped $MoSe_2$ nanostructure could be used as a promising element for sensitive ammonia gas detection.

CRediT authorship contribution statement

Ahmad I. Ayesh: Writing – review & editing, Writing – original draft, Visualization, Validation, Software, Resources, Project administration, Methodology, Investigation, Formal analysis, Data curation, Conceptualization.

Declaration of competing interest

The authors declare that they have no known competing financial interests or personal relationships that could have appeared to influence the work reported in this paper.

Data availability

The raw data required to reproduce these findings are available on request from the author.

Acknowledgement

Open Access funding provided by the Qatar National Library.

References

[1] M. Lashgari, M. Ghanimati, Photocatalytic degradation of H2S aqueous media using sulfide nanostructured solid-solution solar-energy-materials to produce hydrogen fuel, J. Hazard. Mater. 345 (2018) 10–17.
[2] E. Salih, A.I. Ayesh, First principle investigation of H2Se, H2Te and PH3 sensing based on graphene oxide, Phys. Lett. A 384 (2020) 126775.
[3] D. Kwak, M. Wang, K.J. Koski, L. Zhang, H. Sokol, R. Maric, Y. Lei, Molybdenum trioxide (α-MoO3) nanoribbons for ultrasensitive ammonia (NH3) gas detection: integrated experimental and density functional theory simulation studies, ACS Appl. Mater. Interfaces 11 (2019) 10697–10706.
[4] S. Singh, J. Deb, U. Sarkar, S. Sharma, MoSe2 crystalline nanosheets for room-temperature ammonia sensing, ACS Appl. Nano Mater. 3 (2020) 9375–9384.
[5] S.M. Mariappan, M.K. Eswaran, U. Schwingenschlögl, T. Thangeeswari, E. Vinoth, M. Shkir, Z. Said, B. Karthikeyan, Impact of reducing agents on the ammonia sensing performance of silver decorated reduced graphene oxide: experiment and first principles calculations, Appl. Surf. Sci. 558 (2021) 149886.
[6] Y. Yong, F. Ren, Z. Zhao, R. Gao, S. Hu, Q. Zhou, Y. Kuang, Highly enhanced NH3-sensing performance of BC6N monolayer with single vacancy and Stone-Wales defects: a DFT study, Appl. Surf. Sci. 551 (2021) 149383.
[7] M. Chhowalla, H.S. Shin, G. Eda, L.-J. Li, K.P. Loh, H. Zhang, The chemistry of two-dimensional layered transition metal dichalcogenide nanosheets, Nat. Chem. 5 (2013) 263–275.
[8] S. Stankovich, D.A. Dikin, G.H. Dommett, K.M. Kohlhaas, E.J. Zimney, E.A. Stach, R.D. Piner, S.T. Nguyen, R.S. Ruoff, Graphene-based composite materials, Nature 442 (2006) 282–286.
[9] A.I. Ayesh, R.E. Ahmed, M.A. Al-Rashid, R.A. Alarrouqi, B. Saleh, T. Abdulrehman, Y. Haik, L.A. Al-Sulaiti, Selective gas sensors using graphene and CuO nanorods, Sens. Actuators A, Phys. 283 (2018) 107–112.
[10] W. Guo, X. Lu, S. Sun, X. Ye, First-principles study on metal-modified N2P6 nanoscale layers for adsorption performance and sensing capability, ACS Appl. Nano Mater. 5 (2022) 1102–1109.
[11] A.I. Ayesh, H2S and SO2 adsorption on Cu doped MoSe2: DFT investigation, Phys. Lett. A 422 (2022) 127798.
[12] S. Singh, R.C. Singh, S. Sharma, Room temperature ammonia sensing using MoSe2 nanostructures, Mater. Today Proc. 28 (2020) 11–13.
[13] Z. Xiao, W. Wu, X. Wu, Y. Zhang, Adsorption of NO2 on monolayer MoS2 doped with Fe, Co, and Ni, Cu: a computational investigation, Chem. Phys. Lett. 755 (2020) 137768.
[14] J. Wang, Q. Zhou, L. Xu, X. Gao, W. Zeng, Gas sensing mechanism of dissolved gases in transformer oil on Ag–MoS2 monolayer: a DFT study, Physica E, Low-Dimens. Syst. Nanostruct. 118 (2020) 113947.
[15] S. Tongay, J. Zhou, C. Ataca, K. Lo, T.S. Matthews, J. Li, J.C. Grossman, J. Wu, Thermally driven crossover from indirect toward direct bandgap in 2D semiconductors: MoSe2 versus MoS2, Nano Lett. 12 (2012) 5576–5580.
[16] G. Jeevanandham, K. Vediappan, Z.A. ALOthman, T. Altalhi, A.K. Sundramoorthy, Fabrication of 2D-MoSe2 incorporated NiO Nanorods modified electrode for selective detection of glucose in serum samples, Sci. Rep. 11 (2021) 1–13.
[17] T. Liu, Z. Cui, X. Li, H. Cui, Y. Liu, Al-doped MoSe2 monolayer as a promising biosensor for exhaled breath analysis: a DFT study, ACS Omega 6 (2020) 988–995.
[18] S. Ma, L. Su, L. Jin, J. Su, Y. Jin, A first-principles insight into Pd-doped MoSe2 monolayer: a toxic gas scavenger, Phys. Lett. A 383 (2019) 125868.
[19] D. Zhang, Q. Li, P. Li, M. Pang, Y. Luo, Fabrication of Pd-decorated MoSe2 nanoflowers and density functional theory simulation toward ammonia sensing, IEEE Electron Device Lett. 40 (2019) 616–619.
[20] E. Salih, A.I. Ayesh, First principle study of transition metals codoped MoS2 as a gas sensor for the detection of NO and NO2 gases, Physica E, Low-Dimens. Syst. Nanostruct. (2021) 114736.
[21] J. Ge, L. Fan, J. Wang, Q. Zhang, Z. Liu, E. Zhang, Q. Liu, X. Yu, B. Lu, MoSe2/N-doped carbon as anodes for potassium-ion batteries, Adv. Energy Mater. 8 (2018) 1801477.

[22] Y. Kim, S.-K. Kang, N.-C. Oh, H.-D. Lee, S.-M. Lee, J. Park, H. Kim, Improved sensitivity in Schottky contacted two-dimensional MoS2 gas sensor, ACS Appl. Mater. Interfaces 11 (2019) 38902–38909.
[23] Y. Gui, J. Shi, L. Xu, L. Ran, X. Chen, Aun (n = 1–4) cluster doped MoSe2 nanosheet as a promising gas-sensing material for C2H4 gas in oil-immersed transformer, Appl. Surf. Sci. 541 (2021) 148356.
[24] Y. Gui, Y. Chen, X. He, L. Xu, X. Chen, Electronic properties of Ptn (n = 4, 13, 15) nanoclusters decorated MoSe2 monolayer and its effect on C2H2 adsorption: first principles study, Appl. Surf. Sci. 563 (2021) 150375.
[25] H. Luo, Y. Cao, J. Zhou, J. Feng, J. Cao, H. Guo, Adsorption of NO2, NH3 on monolayer MoS2 doped with Al, Si, and P: a first-principles study, Chem. Phys. Lett. 643 (2016) 27–33.
[26] E. Salih, A.I. Ayesh, DFT investigation of H2S adsorption on graphenenanosheets and nanoribbons: comparative study, Superlattices Microstruct. 146 (2020) 106650.
[27] E. Salih, A.I. Ayesh, Enhancing the sensing performance of zigzag graphene nanoribbon to detect NO, NO2, and NH3 gases, Sensors 20 (2020) 3932.
[28] E. Salih, A.I. Ayesh, Computational study of metal doped graphene nanoribbon as a potential platform for detection of H2S, Mater. Today Commun. 26 (2021) 101823.
[29] B. Salah, A.I. Ayesh, Fabrication of H2S sensitive gas sensors formed of SnO2-Fe2O3 composite nanoparticles, Mater. Chem. Phys. (2021) 124597.
[30] E. Salih, A.I. Ayesh, Sensitive SO2 gas sensor utilizing Pt-doped graphene nanoribbon: first principles investigation, Mater. Chem. Phys. 267 (2021) 124695.
[31] A.I. Ayesh, Effect of CuOx additive site to graphene nanoribbon on its adsorption for hydrogen sulfide, Results Phys. 24 (2021) 104199.
[32] J.P. Perdew, K. Burke, M. Ernzerhof, Generalized gradient approximation made simple, Phys. Rev. Lett. 77 (1996) 3865.
[33] S. Grimme, Semiempirical GGA-type density functional constructed with a long-range dispersion correction, J. Comput. Chem. 27 (2006) 1787–1799.
[34] G. Bergman, Influence of spin-orbit coupling on weak localization, Phys. Rev. Lett. 48 (1982) 1046.
[35] E. Salih, A.I. Ayesh, Pt-doped armchair graphene nanoribbon as a promising gas sensor for CO and CO2: DFT study, Physica E, Low-Dimens. Syst. Nanostruct. 125 (2021) 114418.
[36] D. Liu, Y. Gui, C. Ji, C. Tang, Q. Zhou, J. Li, X. Zhang, Adsorption of SF6 decomposition components over Pd (1 1 1): a density functional theory study, Appl. Surf. Sci. 465 (2019) 172–179.
[37] E. Salih, A.I. Ayesh, CO, CO2, and SO2 detection based on functionalized graphene nanoribbons: first principles study, Physica E, Low-Dimens. Syst. Nanostruct. (2020) 114220.
[38] R.S. Mulliken, Electronic population analysis on LCAO–MO molecular wave functions. I, J. Chem. Phys. 23 (1955) 1833–1840.
[39] Y. Zhang, T.-R. Chang, B. Zhou, Y.-T. Cui, H. Yan, Z. Liu, F. Schmitt, J. Lee, R. Moore, Y. Chen, Direct observation of the transition from indirect to direct bandgap in atomically thin epitaxial MoSe 2, Nat. Nanotechnol. 9 (2014) 111.
[40] V. Nagarajan, R. Chandiramouli, MoSe2 nanosheets for detection of methanol and ethanol vapors: a DFT study, J. Mol. Graph. Model. 81 (2018) 97–105.
[41] V.E.C. Padilla, M.T.R. de la Cruz, Y.E.Á. Alvarado, R.G. Díaz, C.E.R. García, G.H. Cocoletzi, Studies of hydrogen sulfide and ammonia adsorption on P- and Si-doped graphene: density functional theory calculations, J. Mol. Model. 25 (2019) 94.
[42] T. Pakornchote, A. Ektarawong, B. Alling, U. Pinsook, S. Tancharakorn, W. Busayaporn, T. Bovornratanaraks, Phase stabilities and vibrational analysis of hydrogenated diamondized bilayer graphenes: a first principles investigation, Carbon 146 (2019) 468–475.
[43] M.G. Ahangari, A.H. Mashhadzadeh, M. Fathalian, A. Dadrasi, Y. Rostamiyan, A. Mallahi, Effect of various defects on mechanical and electronic properties of zinc-oxide graphene-like structure: a DFT study, Vacuum 165 (2019) 26–34.
[44] X. Gao, Q. Zhou, J. Wang, L. Xu, W. Zeng, Adsorption of SO2 molecule on Ni-doped and Pd-doped graphene based on first-principle study, Appl. Surf. Sci. (2020) 146180.
[45] G.K. Walia, D.K.K. Randhawa, First-principles investigation on defect-induced silicene nanoribbons—a superior media for sensing NH3, NO2 and NO gas molecules, Surf. Sci. 670 (2018) 33–43.
[46] W. Hui, G. Chang, W. Gao, Exploring the electronic and magnetic properties of noble metal (Pd, Pt, Au) adsorbed MoSe2 monolayers and their performance towards sensing gas molecules, Physica E, Low-Dimens. Syst. Nanostruct. 122 (2020) 114167.
[47] A.I. Ayesh, A.A. Alyafei, R.S. Anjum, R.M. Mohamed, M.B. Abuharb, B. Salah, M. El-Muraikhi, Production of sensitive gas sensors using CuO/SnO 2 nanoparticles, Appl. Phys. A 125 (2019) 1–8.